JOURNAL OF RESEARCH of the National Bureau of Standards—D. Radio Propagation
Vol. 67D, No. 3, May–June 1963

Effects of Radio Wave Propagation Through Mid-Latitude 6300 A Auroral Arcs

J. R. Roach [1]

(Received November 20, 1962)

Very high frequency radio signals propagated from a polar orbiting satellite through a system of multiple 6300 A red auroral arcs are shown to be strongly perturbed by each arc. The perturbations are characterized by amplitude scintillation of the received signal. The scintillation power correlates logarithmically with the arc photon flux, as derived from the photometric observations. The red arcs and radio scintillations were observed on the night of 12/13 November 1960, during which a major magnetic storm was in process. Similar measurements on the quiet magnetic night of 18/19 February 1961, revealed no appreciable radio scintillation or red arc activity.

1. Introduction

Recent research on mid-latitude 6300 A arcs has shown that they consist of a tube of emission oriented along magnetic isoclines and extending over considerable distances on the Earth's surface. Barbier [1958] and F. E. Roach and Marovich [1959] have presented observations of red arcs that have extended from Haute Provence, France to Fritz Peak, Colo. F. E. Roach, Barbier, and Duncan [1962] have discussed a red arc which appeared almost simultaneously at about the same invariant latitude in the northern and southern hemispheres, and separated by over 150 deg of longitude.

The height of red arc maximum intensity has been established on two occasions as approximately 400 km by F. E. Roach, Moore, Bruner, Cronin, and Silverman [1960]; and by Moore and Odenkrantz [1961]. The general cross section intensity profile has been determined by Tohmatsu and F. E. Roach [1962], based on observations of several red arcs at Fritz Peak, Colo.; revealing a somewhat elliptical tube structure, with maximum intensity centered at 390 km, extending down to 300 km and up to 750 km; and extending 400 km north and south of the center.

These general large-scale characteristics of mid-latitude 6300 A arcs are verified in this paper by independent photometric and radio telescope observations. Photometric data of the 6300 A arc emission were obtained at Fritz Peak, Colo., during a period when observations of satellite signals were made at Van Nuys, Calif. The radio signals were observed to be strongly perturbed as a result of passage through a region in the ionosphere which corresponded in time and space with longitude extensions of red arcs observed at Fritz Peak. The radio signal perturbation is shown to be logarithmically proportional to the arc photon flux.

Data are presented for several orbits on three different nights, for which the magnetic K_p index varied from a maximum of 9° to a minimum of 2^+. Severe radio signal perturbations coincident with 6300 A arcs occurred on the night of 12/13 November 1960 following a major solar flare event. In contrast the observation of a similar satellite radio signal on a geomagnetically quiet night revealed virtually no perturbation, and no 6300 A arcs were observed.

2. Observational Techniques

The data discussed in this paper were independently obtained by the airglow photometers at Fritz Peak, Colo., and by a radio telescope at Van Nuys, Calif. The 6300 A photometric data were obtained with the standard birefringent filter photometer, and the measurement techniques have been discussed by F. E. Roach and Marovich [1959 and 1960] in previous publications. It need only be stated here that 6300 A data were obtained in almucantar sweeps of the photometer every 15 min at zenith angles of 0, 40, 60, 70, 75, and 80 deg.

The radio propagation data were obtained with a research radio telescope which received signals from the polar orbiting satellites. The signal source in the satellites was a VHF communications link utilizing a transmitting antenna with a gain of nominal unity.

The radio telescope was located at the Lockheed Missile and Space Company facility, Van Nuys, Calif., and the 6300 A photometer was located at the National Bureau of Standards facility at Fritz Peak, Colo. The geodetic and geomagnetic coordinates for these stations are given in table 1.

The radio telescope consisted of a trihelix array with a common ground plane, mounted on a servo-

TABLE 1. *Coordinates of observing stations*

Station	Geodetic		Geomagnetic latitude	Elevation above sea-level
	Latitude	Longitude		
Van Nuys, Calif.	34°13′ N	118°29′ W	41.0°	213 m
Fritz Peak, Colo.	39°54′ N	105°29′ W	48.7°	2740 m

[1] Member of the Scientific Staff of Ball Brothers Research Corporation, Boulder Colo.

driven pedestal. The trihelix array was controllable in elevation and azimuth by means of a manually operated console. The receiving antenna had a maximum gain of 19 db, and received the signals as circularly polarized components. The effective ± 3 db antenna beamwidth was 15 deg.

The feeds from the three helices were impedance matched and coupled to a common feed at the input to the preamplifier, mounted on the pedestal. The preamplifier had a gain of 23 db with a noise figure of 3.5 db. The receiver was a Nems Clarke Model No. 1673 operated in the FM detection mode at a 300 kc/s IF bandwidth. The carrier signal frequency was in the communications band from 225 Mc/s to 240 Mc/s. The FM intelligence threshold of the receiver for the composite signal was 108 dbm.

The automatic gain control circuit of the receiver was modified to provide a linear output voltage for a logarithmic power input from 115 dbm to 60 dbm. This AGC voltage was monitored as a measure of the received signal strength in a 10 c/s response circuit, which in turn modulated a voltage controlled subcarrier. The subcarrier frequency was directly recorded on a channel of magnetic tape along with a time standard. The resolution of this monitor was approximately ± 0.1 db.

The entire electronics system was calibrated each orbital acquisition by inserting the output of a standard signal generator in the preamplifier input. The composite FM-FM signal was simulated by means of external oscillators modulating the signal generator carrier at the same deviation ratios as the satellite link. The trihelix array and ground plane were calibrated in a full-scale antenna range.

3. Radio Propagation Data

The radio telescope was in operation during the period, August 1960 to March 1961, and obtained recordings of signals from several polar orbiting satellites. Data were selected for analysis during nighttime passages of the satellites that corresponded with photometric observations at Fritz Peak. Corresponding data were obtained for the nights of 12/13 November 1960 and 18/19 February 1961. Radio propagation data were also analyzed for the night of 7/8 December 1960. The November night was notable for a major geomagnetic storm, and the respective magnetic K_p indices [2] for each night are shown in table 2. Radio propagation data were also reviewed for several other nights to establish that the normal characteristics of the received signals were similar to those observed on the night of 18/19 February 1961.

On each of the three nights of interest in this paper, radio signals were obtained for one orbital pass east and one orbital pass west of the radio telescope. The east and west orbits on each night were in approximately the same positions and passed the radio telescope during a 3-hr period following local midnight. The orbital paths for these nights are shown in geodetic latitude and longitude in figure 1. The respective satellite altitudes and ranges from the radio telescope are shown in table 3.

Continuous recordings of the radio signals were obtained for these orbital passes and portions of the received signal strength for each pass are plotted in figures 2a and 2b. These plotted data are presented for two time periods when the satellite range to the radio telescope was the same north of the telescope as south of it. The ordinate scales represent the received power in decibels with respect to 1 μv at the 50-ohm receiver input.

[2] The magnetic K_p index is the geomagnetic planetary index.

TABLE 2. *Magnetic K indices.*

K_p Index

Date	Universal times		
	6:00	9:00	12:00
12/13 November 1960	9−	9o	9o
7/8 December 1960	5+	4−	4o
18/19 February 1961	2+	3+	3+

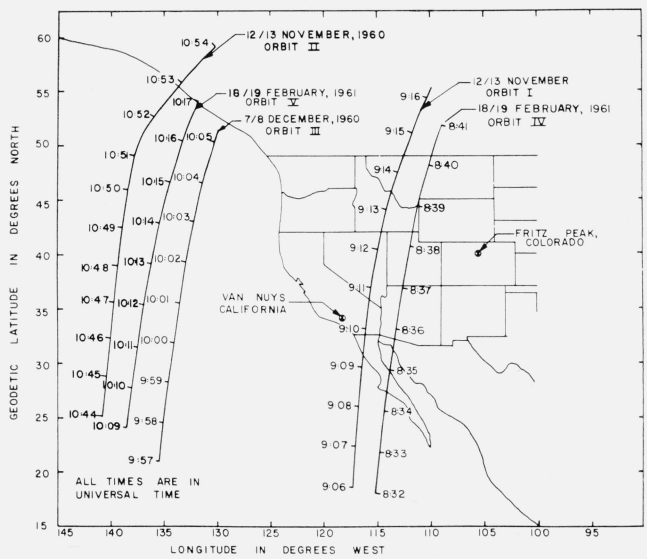

FIGURE 1. *Geodetic latitude and longitude projections of the five satellite orbital paths discussed in this paper.*

Location indicated for Van Nuys, California and Fritz Peak, Colorado. Times indicated on each projection are Universal Time.

TABLE 3. *Satellite altitudes and ranges*

Orbit	Universal time	Altitude	Range
		km	*km*
I	9:06	886	2026
	9:10	830	879
	9:15	735	2216
II	10:44	854	2957
	10:48	785	2610
	10:53	690	3127
III	9:57	619	2554
	10:01	581	1842
	10:06	520	2580
IV	8:32	565	1900
	8:36	505	710
	8:41	430	2280
V	10:08	550	2610
	10:12	490	1800
	10:17	415	2600

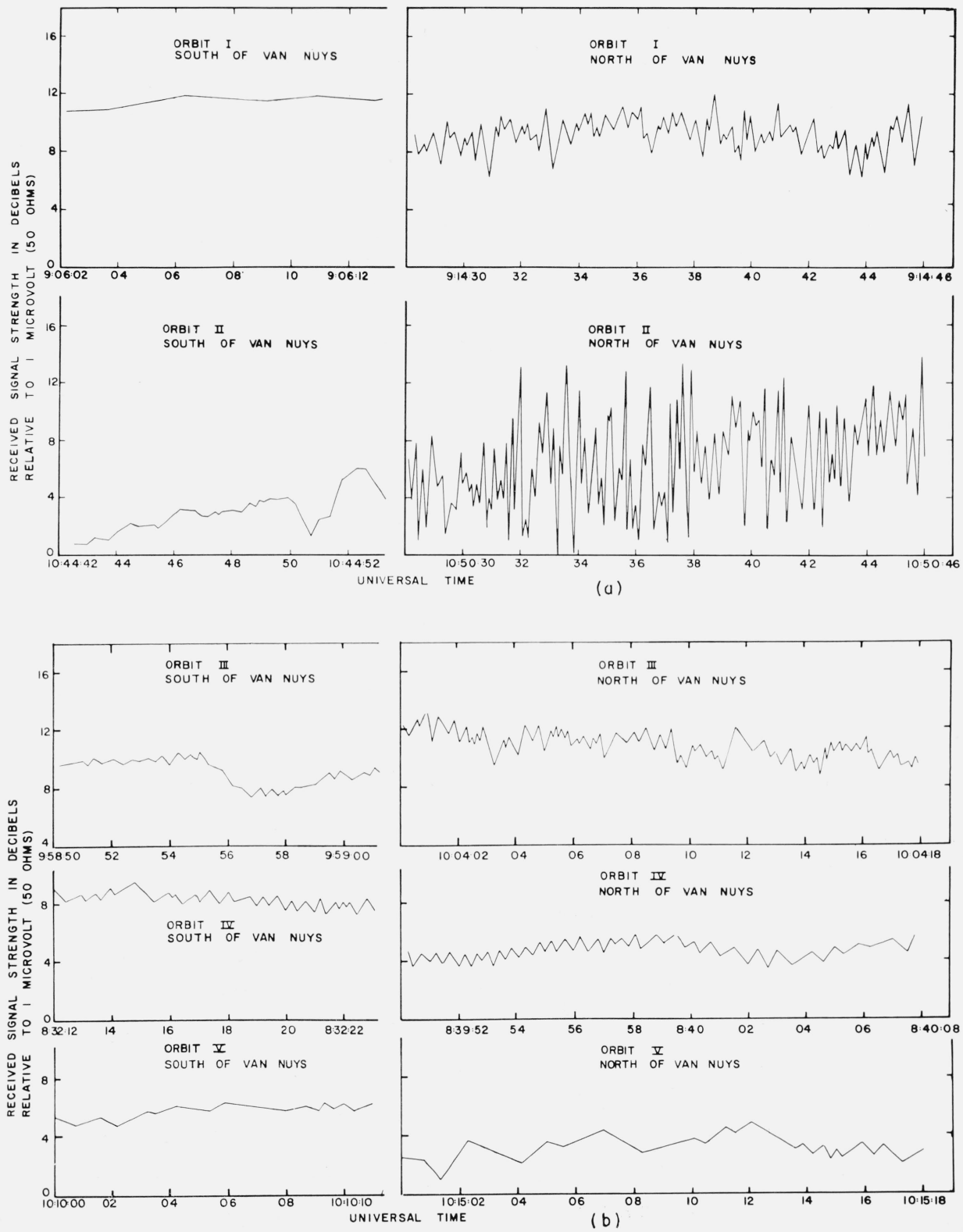

FIGURE 2. *Satellite radio wave signal strength received at the Van Nuys radio telescope for portions of the orbits where the range from the satellite to Van Nuys was the same south as north of the radio telescope.*

(a) Orbits I and II; (b) Orbits III, IV, and V.

4. Photometric Data

Photometric observations of the 6300 A emission were obtained continuously throughout the night of 12/13 November 1960. No observations were made during the night of 7/8 December 1960. Typical almucantar sweeps are presented in figure 3 for the November night at the approximate times of the satellite orbital passes. During the February night the photometric observations were terminated prior to the satellite orbital passes. However, data were obtained up to 7:00 u.t., during which time the 6300 A intensity never exceeded 125 rayleighs.[3] There was no evidence of 6300 A arcs up to 7:00 u.t. in contrast to the well defined arc structure prior to the time on 12/13 November 1960. This is consistent with the relative magnetic activity for the two nights; high activity seems to be required for the arc formation.

In figure 3, evidence for three red arcs is shown for 9:10 u.t. and 10:55 u.t. Arcs A and B were in a state of rapid evolution during the period around local midnight. Intensity and position variations were observed between successive 15-min intervals, particularly in the northern regions. The observed position and intensities of arcs A and B are shown in figure 4. The intensities were averaged for the east and west observations on the 75-deg almucantar. Arc C had relatively weak intensity and moved only slightly south during this period.

[3] The rayleigh is defined as a photometric unit where: 1 rayleigh = 10^6 photons/-cm^2 (column) sec.

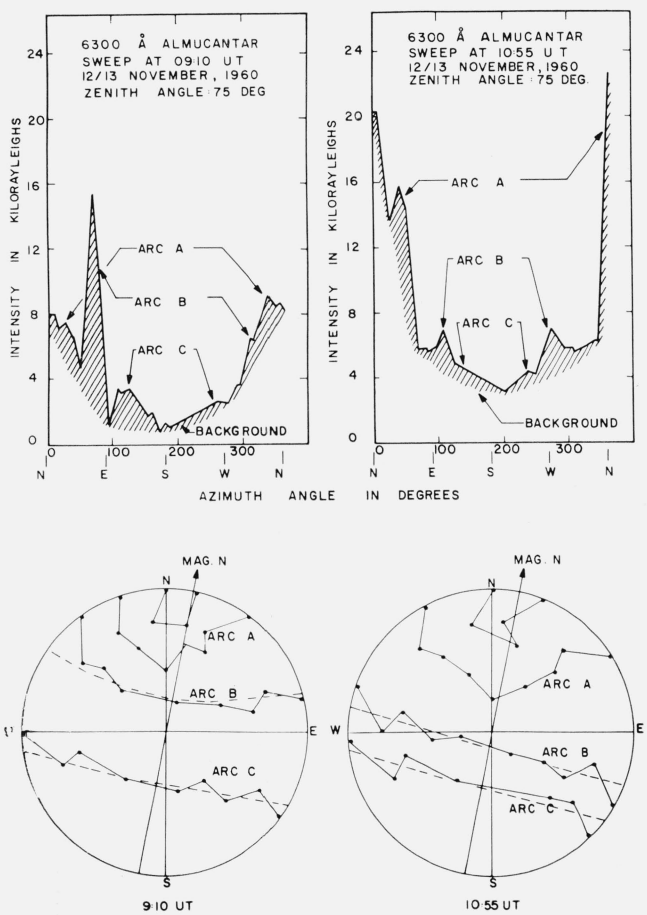

FIGURE 3. *Photometric data of the 6300 A emission observed at Fritz Peak.*

Upper: 75 degree almucantar sweeps for the times of orbits I and II with the three arcs indicated; Lower: circle map presentation of arc indications for each almucantar sweep at the times of orbits I and II. Data points represent the positions of relative peak intensities seen in the upper portion of figure. Sawtooth appearance of data due to hysteresis in the photometer drive mechanism. The circle diameter is 1325 kilometers.

It can be seen from figure 4 that, at the time of orbit I, the arc systems were to the north of Fritz Peak and at low peak intensities. Between orbit I and orbit II the arcs oscillated through an intensity increase of almost an order of magnitude and migrated far to the south from their previous positions. At the time of orbit II, arcs C, B, and A were approximately 5 deg south, 1 deg south, and 3.5 deg north of Fritz Peak respectively. The relative intensity of arc A was approximately twice that of arc B, and arc B was approximately four times the intensity of arc C.

It should be noted that arcs A, B, and C have been described as monochromatic 6300 A emissions. The 5577 A photometric data for the same night indicate that a green arc was in evidence. This arc remained in the general region of red arc A throughout the time spanned by orbits I and II (assuming a 400-km altitude of maximum intensity). The green arc increased in intensity in the same manner as the red arcs at 9:40 u.t. The red arc emissions were generally 1.7 times as intense as the 5577 A emission.

The occurrence of green arcs contiguous with red arcs is so rare that little is known of their altitude or spatial distribution. Therefore, the green arc of 12/13 November 1960, is not included in the analysis presented in this paper, but is left for further investigation.

5. Analysis of the Data

Scintillation of radio signals propagated through the ionosphere is associated with variations in the electron distribution in the ionosphere. It has been suggested by King and F. E. Roach [1961], that the excitation of 6300 A is related to the electron concentration in the F region. A search for a correlation between the two phenomena is therefore in order.

Arcs A, B, and C were extended from the Fritz Peak meridian, along lines of constant invariant latitude,[4] to the longitude of the satellite. The extended arcs are shown in figure 5, and it can be seen that the propagation path of the satellite signal must pass through the arcs. The Fritz Peak meridian positions of both arcs were determined from the data presented in figure 4, for the times of orbits I and II. The root-mean-square (rms) value of the logarithmic power amplitude of the signal

[4] Actually the arcs are more closely alined to parallels of constant sheet parameter L than to magnetic isoclines. The invariant latitude is determined from the sheet parameter L as: $\cos^2\wedge = \frac{R}{L}$; where: $\wedge$ is the invariant latitude; R is the equatorial radius of the Earth; and L is the equatorial radius of the line of force.

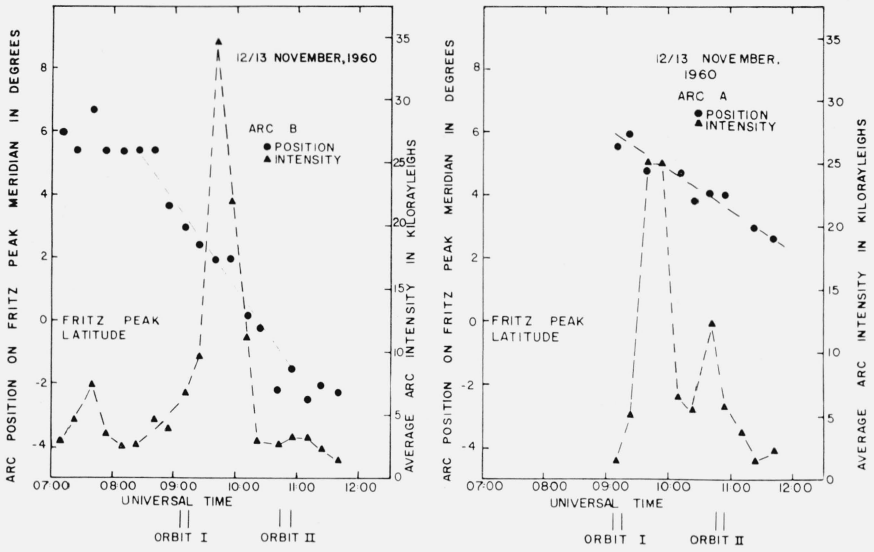

FIGURE 4. *Position and intensity of red arcs* A *and* B *during the local early morning of 13 November 1960.*

The time of satellite signal reception at Van Nuys is indicated for orbits I and II. The dashed lines are for clarity.

with respect to the average received signal strength was used as a statistical index of scintillation. The rms values were computed over 3-sec periods and included a fixed sample size of 31 data points. The average signal level was obtained by means of a visual fairing of the plotted signal strength. A nominal 2-sec time constant was applied during the fairing to remove, as much as possible, the manmade variations arising from manual telescope tracking and oscillation of the satellite.

The rms scintillation data are presented as a function of time in figure 6 for the orbits on the three nights. It should be noted that the minimum rms value that could be resolved with the manual data processing techniques used was 0.1 db. For the night of 18/19 February 1961, the rms value exceeded 0.5 db at only one time when it reached 0.7 db. However, on the nights of 12/13 November and 7/8 December, the rms values reached several significant peaks. Restricting the analysis for the present to the night of 12/13 November, let us examine these peaks.

During orbit I the rms index reached maxima of 0.55 db at 909.0 u.t.; 0.49 db at 912.2 u.t.; 1.40 db at 914.7 u.t. and of 1.80 db at 915.1 u.t. These have been identified as peaks d_1, c_1, b_1, and a_1 respectively. Maxima reached during orbit II were 1.40 db at 1047.5 u.t.; 0.85 db at 1049.0 u.t.; 2.60 db at 1050.7 u.t.; and 3.95 db at 1052.4 u.t. identified as peaks d_2, c_2, b_2, and a_2 respectively in figure 6.

The propagation paths corresponding to four of these maxima are projected on the latitude-longitude plot of figure 7. The extended arcs A, B, and C are also shown. The two-dimensional properties of the plot are expanded to the three-dimensional features of the satellite orbit, as well as the propagation paths and the red arcs, by also projecting the loci of constant altitude for the propagation path, as the satellite passes the radio telescope. Shown in figure 7 is the locus altitude of 400-km only.

It is immediately obvious for orbit II that there is a space time coincidence between the 400-km red arcs A, B, and C and the 400-km locus of the propagation paths for peaks a_2, b_2, and c_2. For orbit I, a similar coincidence exists for arcs A, B, and C with peaks a_1, b_1, and c_1, but it is difficult to see since the projections nearly overlap and therefore is not shown.

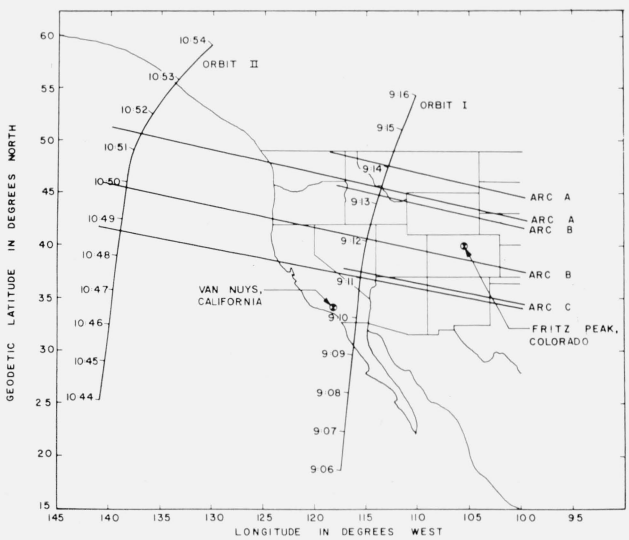

FIGURE 5. *Geodetic latitude and longitude projections of red arcs* A, B, *and* C, *extended from the Fritz Peak meridian position along parallels of constant sheet parameter* L.

Arc positions were determined for the times of orbits I and II, and are shown extended to include the longitude of both orbital passes.

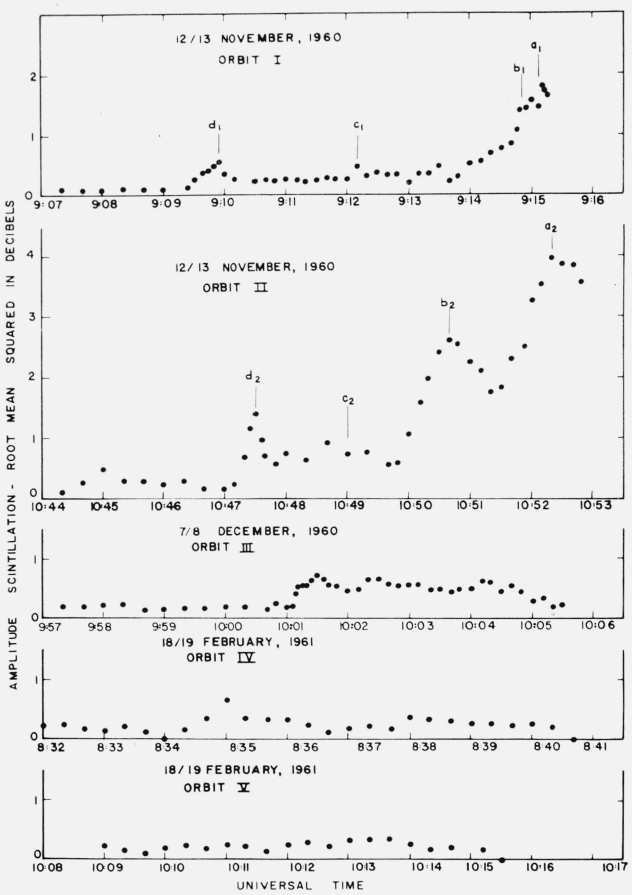

FIGURE 6. *Satellite radio signal perturbations observed at Van Nuys, for each of the five orbits discussed in this paper.*

Expressed as the root-mean-square statistic of the received signal logarithmic power amplitude scintillation. Significant maxima are indicated by lower case letters with a numerical subscript designating the respective orbit.

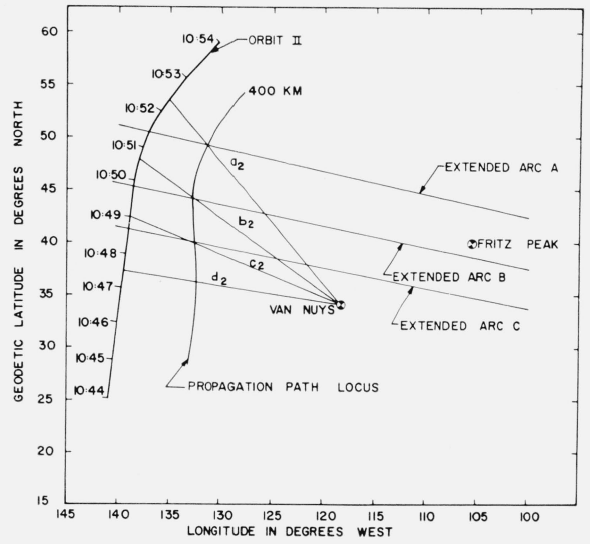

FIGURE 7. *Geodetic latitude and longitude projections of: Extended red arcs* A, B, *and* C; *orbit II; the radio wave propagation path 400 km locus; and the radio wave scintillation maxima propagation paths* a_2, b_2, c_2, *and* d_2.

To avoid confusion, the propagation path loci and scintillation maxima paths for orbit I are not shown.

On the basis of these six space-time correlations it can be stated that the radio signal scintillation is probably associated with a perturbing characteristic accompanying the red arcs.

Looking at the rms data for the night of 7/8 December 1960, three small maxima of 0.73, 0.70, and 0.63 are seen at 1001.5 u.t., 1002.4 u.t., and 1004.2 u.t. respectively. Since no photometric data are available for this night, it can only be conjectured that one or two of these maxima may be associated with red arcs. This seems reasonable since, from table 2, it can be seen that considerable magnetic activity did occur on 7/8 December; but not as intense as on 12/13 November. It is consistent that the radio scintillations for orbit III would be less for the decreased magnetic activity. This argument can be extended to the night of 18/19 February 1961. During this night the magnetic K_p index never exceeded 3+, and it could be expected that the radio scintillations would be near a minimum. As shown in figure 6 for orbits IV and V, the rms value is consistently less than 0.5 db.

6. Further Analysis of the Results

In the preceding section it was shown that radio scintillation peaks *a*, *b*, and *c* correlated with red arcs *A*, *B*, and *C* respectively for both orbits I and II. The positions of these three arcs are shown in table 4 in terms of the *L* parameter. Established by McIlwain [1961], *L* defines the equatorial crossing of the magnetic shell that intersects the 400 km altitude at the arc invariant latitudes. Two additional arcs have been included in this table which require clarification.

Arc *Z* can be discriminated in figure 3 north of arc *A*. It has relatively low intensity and its position is difficult to determine accurately due to its distance from Fritz Peak. However, the position of arc *Z* was estimated from the almucantar data, and is shown in table 4 to extend the data of this multiple arc system.

TABLE 4.—*Arc positions in terms of the sheet parameter L*

Arc	Orbit I		Orbit II	
	L	Δ*L*	*L*	Δ*L*
Z	3.85		3.45	
		0.45		0.62
A	3.20		2.83	
		.43		.55
B	2.77		2.28	
		.76		.31
C	2.01		1.97	
		.24		.22
D	1.77		1.75	

In addition, arc *D* has been included as a probable arc. The existence of arc *D* cannot be verified from the photometric data since it is positioned beyond the field of view of the Fritz Peak photometers. However, it was inferred from radio scintillation peaks d_1 and d_2, on the basis of the excellent correlations between the arcs and the peaks discussed in

the preceding section. The position of arc D was obtained from the invariant latitude at the time of the maximum rms indication.

Included in table 4 is a tabulation of the separation in terms of L, between the arcs. A definitive study of multiple arcs in general is planned.

Let us now examine the properties of the signals propagated through the red arcs. The scintillation peaks were not sharp, but increased to the maximum, and then decreased over a considerable portion of the orbits. Recalling that Tohmatsu and F. E. Roach [1962] have shown that the red arcs extend with decreasing intensity at least 400 km north and south of the center, and from 300 km to 700 km in altitude, the broad scintillation peaks are consistent with the association between arcs and peaks emerging from this study.

In figure 8 the red arc intensity profile has been projected on a latitude-longitude plot, utilizing the propagation path loci to provide the altitude dimension. Arc A and B slant profiles for orbit II are shown and it can be seen that they overlap in the middle. To avoid confusion, the slant profile for arc C was not shown. Similarly, the slant profiles for orbit I have been examined in detail, where the radio signal passed through the arc nominally perpendicular to the tube structure. Each of these slant profiles was numerically integrated to yield the photon flux coincident with the propagation paths.

The integrations were based on a maximum intensity for the longest path length through the center of intensity. The maximum intensity was assumed to be equal to the arc emission intensity observed at Fritz Peak. The zenith angles of the photometer axis were nearly the same as those of the radio telescope axis, so that this assumption is sufficiently accurate to provide an order of magnitude value for the number of column photons.

The number of photons along the propagation paths was computed according to the relative intensities within an arc and the integrated path lengths. These data are shown in figure 9, plotted with the amplitude scintillation rms data. The scintillation data in decibels had a baseline which varied between 104 dbm and 100 dbm throughout the region of the arc perturbation.

Since the profiles of arc A, B, and C extend into each other, the total integrated photon flux includes the sum of the contributions of each arc. It can be seen in figure 9 that the scintillation power, or the perturbation of the radio signal, was covariant with the integrated photon flux throughout the three regions of arc activity.

A slant profile was also integrated for arc D at its deduced orbit II position, and the correlation between scintillation peak d_2 and photon flux is shown in figure 9. The intensity of the arc was

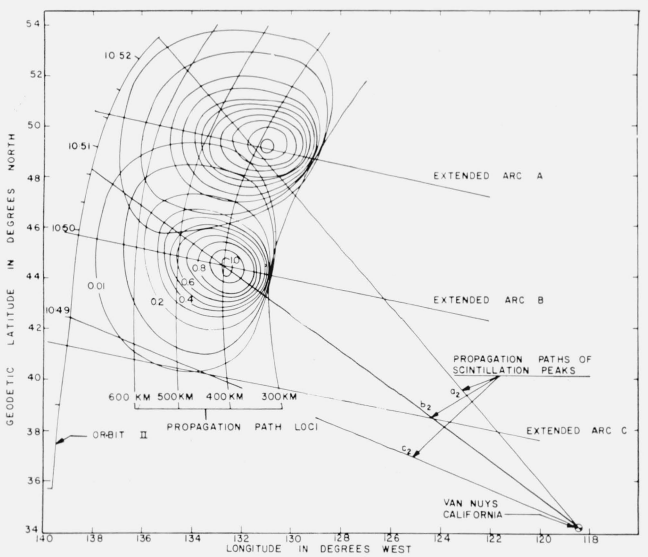

FIGURE 8. *Geodetic latitude and longitude projections of: Orbit II; extended arcs* A, B, *and* C; *the radio wave propagation path loci; the radio wave scintillation maxima propagation paths; and the slant intensity profiles of arcs* A *and* B.

The relative intensities within the arc are indicated for the profile of arc B, with the maximum relative intensity of 1 shown at the intersection of the extended arc with the 400 km locus of the propagation path coincident with scintillation maximum b_2.

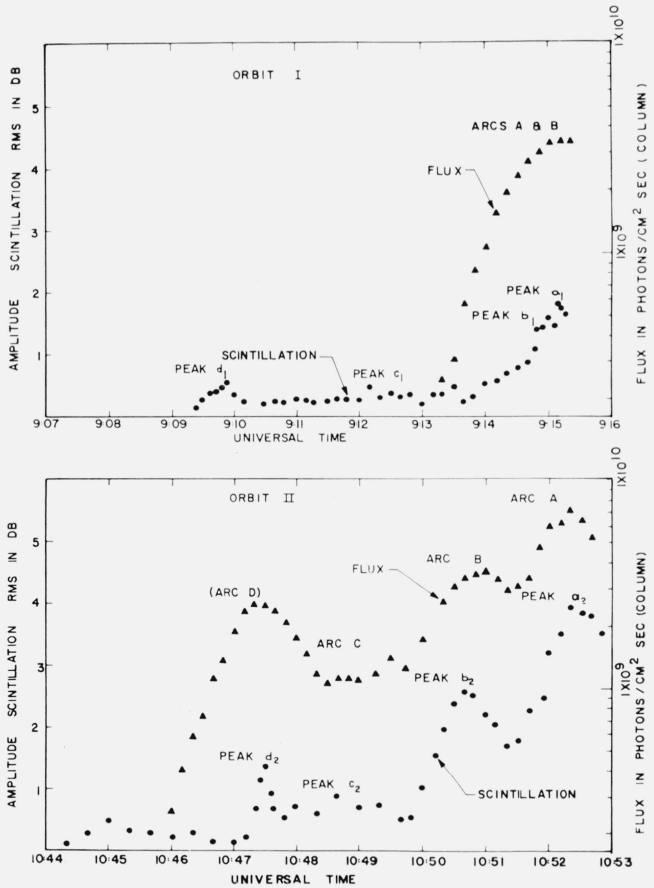

FIGURE 9. *Satellite radio wave scintillation and 6300 A arc column photon flux as a function of the time of orbit I and II radio reception at Van Nuys.*

The 6300 A photon flux was integrated for columns through the arcs according to the slant intensity profiles coincident with the scintillation maxima, and from peak intensities observed at Fritz Peak.

inferred from the relationship between integrated photon flux and scintillation power for the peaks coincident with arcs A, B, and C. Scintillation peak d_2, is quite sharply defined but the photon flux profile obtained was typically extended 400-km north and south of the arc center. This lack of profile correlation may be attributable to a more confined intensity gradient within the arc. That is, the effective north and south ellipticity of the tube may have been reduced by as much as a factor of two.

7. Discussion

The perturbation of VHF radio signals propagated through a red arc, has been shown to correlate with the number of 6300 A photons created along the propagation path. It is, therefore, interesting to examine this relationship with respect to other observations that have shown correlation with red arc phenomena.

King and F. E. Roach [1961] have reported a correlation between a red arc and oblique ionosonde echoes. They found that the f_0F_2 maximum frequency was lower in the oblique echo than in the vertical echo. This indicated that the electron density in the arc was less than in the vertical direction. Referring to figure 4 of King and F. E. Roach [1961], King [1962] reports that from the apparent spread in the oblique return, it can be concluded that the *irregularities* in electron density in the arc were twice as intense as in the vertical direction. King points out that this spread is typical of returns from red arcs. It is, therefore, not surprising to find a clear correlation between red arcs and VHF scintillation.

To aid in the quantitative evaluation of the possible electron structure within the arcs in relation to the 6300 A photon flux, the data from figure 9 are cross plotted in figure 10 so as to provide the scintillation rms as well as the relative scintillation power as a function of integrated photon flux. The relative scintillation power is determined from the logarithmic relationship of the decibel ratio, where the reference power was set equal to one. The functional dependence of scintillation rms on the arc integrated photon flux, as obtained from these data is:

$$S_{rms}=5.32\times \log F-0.66 \qquad (1)$$

where: S_{rms} is the scintillation rms in decibels, F is the arc integrated photon flux in 10^9 photons/cm^2 sec (column); (kilorayleighs).

Equation (1) can also be expressed as the dependence of relative scintillation power on the arc integrated photon flux:

$$S_{sp}=0.86 \times F^{0.53} \qquad (2)$$

where: S_{sp} is the relative scintillation power,
F is the arc integrated photon flux in 10^9 photons/cm^2 sec (column); (kilorayleighs).

From (1) and (2), it can be seen that the radio wave scintillation is logarithmically proportional to the integrated photon flux within the 6300 A arc. It may be speculated that the electron irregularities within the arc leading to scintillations, together with the decrease in electron density are due to a flow of electrons constituting an electric current. Such a flow of electrons might have the double effect of (a) introducing irregularities into the ionospheric plasma through current instabilities, and (b) enhancing the excitation of the oxygen atoms because of the electron "heating" resulting from the current.

The magnetic control of such a current may arise from the outer radiation (Van Allen) zone, as evidenced by the detection of narrow intense zones of radiation at 1000 km over a 6300 A arc, as reported by O'Brien, Van Allen, F. E. Roach, and Gartlein [1960]. The peak of the outer radiation zone does seem to move equatorward to the vicinity of $L=3$ during times of magnetic activity, in apparent agreement with the southward movement of arcs A and B. It has been suggested by Stolov [1962] that mid-latitude 6300 A arcs are associated with the E_2 branch of the outer zone, which remains at relatively constant position, similar to arcs C and D.

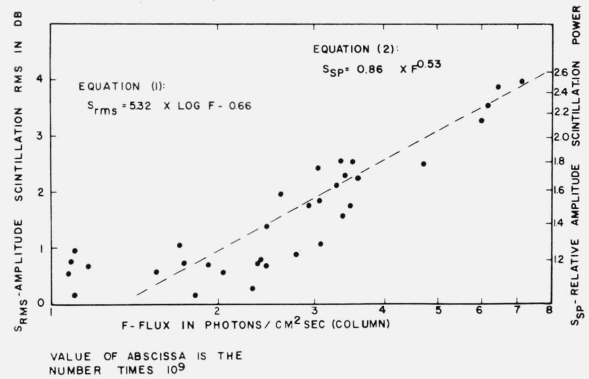

FIGURE 10. *Satellite radio wave scintillation rms and relative power as a function of the integrated arc photon flux.*

The correlation is indicated by the dashed line and eqs (1) and (2) express this relationship.

8. Summary

Very high frequency radio signals, propagated from an orbiting satellite through a system of 6300 A mid-latitude arcs, were shown to be considerably perturbed, as measured by the amplitude scintillation of the receiver signal. Scintillation maxima occurred in space-time coincidence with three red arcs for two successive orbital passes of the satellite. At the time of these correlations, the red arcs measured several kilorayleighs in brightness, as a probable by-product of the major magnetic storm that reached a K_p of 9$_0$ during this period.

The radio scintillation rms was shown to be covariant with the intensity gradients of five arc positions. The intensity gradients of a sixth arc position, below the optical horizon of the Fritz Peak photometer, but inferred from a sharp increase in scintillation rms, probably occurred over a smaller geometrical tube.

The relative scintillation power associated with the arcs was shown to be logarithmically proportional to the columnar photon flux observed photometrically. The low frequency spread and the lower f_0F_2 in the red-arc oblique echo observed in ionogram data can be considered with the scintillation data presented here, to indicate that considerable electron irregularities exist within a 6300 A arc.

It is suggested that red arcs may be due to current systems which redistribute electrons irregularly along the arc tube to cause the increased scintillation, as well as increase the temperature of the electrons to cause the enhanced 6300 A emission. The magnetic control of such a current may arise from the E_2 and E_3 branches of the outer radiation zone.

I thank Dr. F. E. Roach of the National Bureau of Standards, Boulder, Colorado, for making the 6300 A photometer data available for this analysis, and for his valuable counsel and advice in this problem. The radio propagation data were obtained under the Lockheed Missile and Space Company contract AF 04(647)–558. Many people assisted in the acquisition of the radio data, and I would like to acknowledge in particular the work of V. Beelik, V. Counter, D. Klein, H. Louch, F. Munson, and A. Palentonio. The balance of the preparation of this paper was unsupported; but I would like to thank the Control Data Corporation, Denver office, for assisting in the programing and for providing computer time during this analysis; as well as Ball Brothers Research Corporation for aid in the graphic presentation of the information and for publication services.

9. References

Barbier, D. (1958), L'activite aurorale aux bases latitudes' Ann. Geophys. **14,** 334.

King, G. A. M. (25 Oct. 1962), Private communication.

King, G. A. M., and F. E. Roach (1961), Relationship between red auroral arcs and ionospheric recombination, J. Res. NBS **65D,** (Radio Prop.) No. 2, 129–135.

McIlwain, C. E. (1961), Co-ordinates for mapping the distribution of magnetically trapped particles, J. Geophys. Res. **66,** 3681–3691.

Moore, J. G., and F. K. Odenkrantz (1961), The height and geographical position of the red auroral arc of April 1–2, 1960, J. Geophys. Res. **66,** 2102–2104.

O'Brien, B. J., J. A. Van Allen, F. E. Roach, and C. W. Gartlein (1960), Correlation of an auroral arc and a subvisible monochromatic 6300 A arc with outer-zone radiation on November 28, 1959, J. Geophys. Res. **65,** 2759–2765.

Roach, F. E., and E. Marovich (1959), A monochromatic low latitude aurora, J. Res. NBS **63D,** (Radio Prop.) No. 3, 297–301.

Roach, F. E., and E. Marovich (1960), Aurora of October 22–23, 1958, at Rapid City, South Dakota, J. Res. NBS **64D,** (Radio Prop.) No. 2, 205–209.

Roach, F. E., J. G. Moore, E. C. Bruner, H. Cronin, and S. M. Silverman (1960), The height of maximum luminosity in an auroral arc, J. Geophys. Res. **65,** 3575.

Roach, F. E., D. Barbier, and R. A. Duncan (1963), Observation of a 6300 A arc in France, United States, and Australia, Ann. Geophys. (in press).

Stolov, H. L. (1962), Bifurcation of the outer Van Allen belt and related auroral phenomena, J. Geophys. Res. **67,** 404–406.

Tohmatsu, T., and F. E. Roach (1962), The morphology of mid-latitude 6300 Angstrom arcs, J. Geophys. Res. **67,** 1817–1821.

(Paper 67D3–261)

672865—63——2